

ARTICLE

Elucidating the Chemiexcitation of Dioxetanones by Replacing the Peroxide Bond with S-S, N-N and C-C Bonds

Carla M. Magalhães,^a Patricia González-Berdullas,^a Joaquim C.G. Esteves da Silva^{a,b} and Luís Pinto da Silva^{*a,b}

Received 00th January 20xx,
Accepted 00th January 20xx

DOI: 10.1039/x0xx00000x

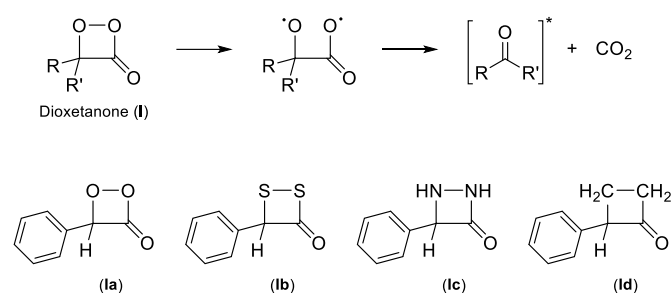
Dioxetanone is one of the prototypical cyclic peroxide intermediates in several chemiluminescent and bioluminescent systems, in which thermolysis reactions allow for efficient singlet chemiexcitation. While the chemiexcitation mechanism of dioxetanone and peroxide intermediates it still far from understood, the presence of a peroxide bond that undergoes bond breaking has been found to be a constant. Here we have addressed the following questions: can other non-peroxide bonds lead to chemiexcitation and, if not, can the differences between dioxetanone and non-peroxide derivatives help to elucidate its chemiexcitation mechanism? To this end, we have used a reliable TD-DFT approach to model the thermolysis and chemiexcitation of a model dioxetanone and three other non-peroxide derivatives. The results showed that only the dioxetanone molecule should lead to chemiluminescence, as it is the only one for which thermolysis is energetically favorable and provides a pathway for singlet chemiexcitation. Finally, the chemiexcitation of the model dioxetanone is explained by its access, during thermolysis, to a biradical region where the ground and excited states are degenerated. This occurs due to an increased interaction between the reaction fragments, which extends the biradical regions and delays the rupture of the peroxide ring.

1. Introduction

Chemiluminescence (CL) is the conversion of thermal energy into excitation energy during a chemical reaction, leading to light-emission.¹⁻⁴ Bioluminescence (BL) is a subtype of CL, as it consists of the same general phenomenon, but involving an enzyme-catalysed reaction in living organisms (such as fireflies, fishes, fungi, and earthworms, among others).⁵⁻⁷ Given that light-emission occurs without photo-excitation, CL and BL systems are characterized by a diminished possibility of autofluorescence arising from the background signal.^{8,9} Therefore, both CL and BL systems have been gaining several applications in field of sensing,^{10,11} *in vitro/in vivo* real-time imaging,¹²⁻¹⁴ and even as self-activating sensitizers for cancer therapy.¹⁵⁻¹⁷

Generally, CL and BL occur via a two-step process: oxidation of the reactant toward the generation of an unstable and energy-rich peroxide intermediate; and subsequent thermolysis of the peroxide intermediate, which allows for the thermally-activated singlet ground state (S_0) reaction to produce an oxidized reaction product in the first singlet excited state (S_1), leading to

singlet chemiexcitation.¹⁸⁻²² Chemiexcitation can also lead to the generation of chemiluminophores in their first triplet excited state (T_1).^{1-3,17} However, as phosphorescence is easily quenched in solution, peroxide-based CL and BL result from S_1 chemiluminophores.



Scheme 1 – Schematic representation of the thermolysis and chemiexcitation mechanism of typical dioxetanones (top). Molecular structures of the model phenyl-substituted dioxetanone **1a** and its non-peroxide derivatives **1b-d** (bottom).

Dioxetanone (**Scheme 1**) is a ubiquitous type of CL/BL-capable cyclic peroxide, as it is responsible for chemiexcitation in several CL (acridinium esters and 2-coumaranones)²³⁻²⁶ and BL systems (fireflies, Coelenterazine, *Cypridina* luciferin, and earthworm *Fredericia heliota*).²⁷⁻³⁰ Despite significant research effort into this and other CL/BL-capable peroxides, the mechanism that governs efficient singlet chemiexcitation is still not clear.

Efficient singlet chemiexcitation was initially explained by both inter- and intramolecular Chemically Induced Electron-Exchange Luminescence (CIEEL) mechanisms,^{31,32} consisting in

^a Chemistry Research Unit (CIQUP), Faculty of Sciences of University of Porto (FCUP), Rua do Campo Alegre 697, 4169-007, Porto, Portugal.

^b LACOMEPHI, GreenUPorto, Faculty of Sciences of University of Porto (FCUP), Rua do Campo Alegre 697, 4169-007, Porto, Portugal.

*e-mail: luis.silva@fc.up.pt

† Footnotes relating to the title and/or authors should appear here.

Electronic Supplementary Information (ESI) available. See DOI: 10.1039/x0xx00000x

an electron transfer (ET) from an electron-rich group to the peroxide with formation of a radical ion pair. The radical ion pair undergoes back ET (BET), which leads to efficient chemiexcitation due to charge annihilation. However, more recent re-evaluations of model CIEEL systems by other authors revealed significantly lower quantum yields than the values previously reported and used to justify the CIEEL mechanism.^{33,34}

Thus, the basis on which CIEEL was developed was proven incorrect and this prompted researchers to try to modify the mechanism, which resulted in the development of the Charge Transfer-Initiated Luminescence (CTIL) mechanism. In it, the efficient singlet chemiexcitation is attributed to a more gradual charge transfer (CT) and back charge transfer (BCT) between an ionized electron-rich group and the peroxide, instead of full ET/BET with formation of radical ion pairs.³⁵⁻³⁸ Unfortunately, even this revised version of CIEEL was unable to account for different experimental and theoretical results associated with the CL/BL reaction of different dioxetanones.

On the one hand, theoretical calculations have shown that neutral imidazopyrazinone-based dioxetanones present more efficient singlet chemiexcitation than their anionic counterparts.³⁹⁻⁴³ This results from the access of these neutral peroxides to a large and flat potential energy surface (PES) region with biradical character, in which S_0 and S_1 states are degenerated. The degeneracy between states for a large part of the PES increases the probability for efficient transition between states. On the other hand, ionic dioxetanones were not found to have access to this region and their $S_0 - S_1$ energy gap values within the biradical region were higher than for neutral dioxetanones, also indicating a lower chemiexcitation efficiency.³⁹⁻⁴³ As neutral dioxetanones present higher singlet chemiexcitation efficiencies than their ionic counterparts, this questions the need of ionizable groups for efficient chemiexcitation stated in the CTIL mechanism. These results and conclusions were supported experimentally for CL-capable imidazopyrazinones.^{39,41,44-46} Finally, the analysis of different studies indicates that there is no clear relationship between ET-BET/CT-BCT and efficient chemiexcitation, as there are instances of dioxetanones with less efficient chemiexcitation decomposing with significant ET-BET/CT-BCT, while dioxetanones with more efficient chemiexcitation decompose with either relevant or non-relevant ET-BET/CT-BCT.^{35,37,39,40-43}

In conclusion, and despite decades of research, it is still not clear what is the mechanism that allows for efficient chemiexcitation. Without this knowledge, it is quite difficult to develop, in a target-oriented manner, innovative CL/BL systems, with enhanced properties, to be used in novel and/or existent applications with optimized performance.

Typical CL systems undergo chemiexcitation by thermolysis of peroxide intermediates (either in linear or cyclic form), such as dioxetanone, which highlights the importance of the peroxide (O-O) bond for chemiexcitation (**Scheme 1**).¹⁻³ However, this raises the question: can other bond types also lead to efficient chemiexcitation? While four-membered heterocyclic molecules

have been the focus of some research,^{47,48} they are still unexplored in terms of CL studies.⁴⁹

Herein, we have evaluated the chemiexcitation reaction of a model dioxetanone and other non-peroxide derivatives. Our objective here is twofold: assess if non-peroxide four-membered heterocyclics can also undergo chemiexcitation; and if not, understand which features of the peroxide-containing dioxetanone allow for chemiexcitation through a comparative analysis. Such information is essential to clarify the doubts regarding the mechanism behind efficient chemiexcitation. To this end, an efficient and reliable time-dependent (TD) density functional theory (DFT) approach was employed, which was already extensively validated in previous studies.^{15,30,39-43} More specifically, TD-DFT calculations were used to characterize the chemiexcitation reaction of a model dioxetanone and three non-peroxide derivatives (**Scheme 1**). The model dioxetanone system (**1a**) is composed of a four-membered peroxide ring which is connected to an electron-rich moiety (phenyl group) given the relevance of electron-rich groups in CIEEL and CTIL theories.^{31,32,35-38} The derivatives consist of similar structures in which the peroxide bond (-O-O-) is replaced by either a -S-S- (**1b**) bond, a -HN-NH- (**1c**) bond or a -H₂C-C₂H-bond (**1d**).

2. Computational Methods

The geometries and frequency calculations of the S_0 state of model dioxetanone (**1a**) and derivatives (**1b-1d**) (**Scheme 1**) were calculated at the ω B97XD/6-31G(d,p) level of theory,⁵⁰ with an open-shell (U) approach for transition states (U) and a closed-shell one (R) for reactants/products. Broken-symmetry (BS) technology was also used with the U approach to make an initial guess for a biradical by mixing HOMO and LUMO.^{35-37,39,41,44-46} IRC calculations were performed to determine whether the calculated transition states (TSs) connect with expected reactants and products. The cartesian coordinates of the calculated TSs for the four studied systems are present in Tables S1-S4. The energies of the S_0 IRC-obtained structures were re-evaluated by single-point calculations at the ω B97XD/6-31+G(d,p) level of theory. The S_1 state was calculated by using a TD-DFT approach at the TD ω B97XD/6-31+G(d,p) level of theory. ω B97XD is a long-range-corrected hybrid exchange-correlation functional that provides accurate estimates for $\pi \rightarrow \pi^*$ and $n \rightarrow \pi^*$ local excitations, and CT and Rydberg states.⁵¹ Furthermore, ω B97XD and other long-range-corrected hybrid exchange-correlation density functionals have been used with success for different dioxetanone systems.^{35,37,39,40-43} All calculations were performed *in vacuo*. The theoretical protocol which was followed was already used with success in the study of several dioxetanone-based reactions.^{15,30,39-43} Calculations were made with the Gaussian 09 program package.⁵²

Table 1 - $\nabla^2 \rho(r)$, $\rho(r)$, ϵ , and $-(G(r_b)/V(r_b))$ values for the O-O/S-S/HN-NH/H₂C-CH₂ BCP for the model dioxetanone (**1a**) and its 3 non-peroxide derivatives (**1b-d**), at the ω B97XD/6-31+G(d,p) level of theory.

	1a	1b	1c	1d
$\nabla^2 \rho(r)$	-0.096	-0.092	-0.501	-0.491
$\rho(r)$	0.279	0.131	0.294	0.231
$-(G(r_b)/V(r_b))$	0.472	0.387	0.344	0.242

3. Results and Discussion

The first step of this work was to analyse the O-O/S-S/HN-NH/H₂C-CH₂ bonding of the four studied compounds (**1a-d**), by using the quantum theory of atoms in molecules (QTAIM) analysis. This methodology identifies the coordinates of a particular type of saddle-point in the electron density distribution, which is known as a bond critical point (BCP). Two of the electronic properties at the BCP are usually employed to characterize the bonding nature in this region: the value of electron density distribution ($\rho(r)$) and the Laplacian $\nabla^2 \rho(r)$. Negative values of $\nabla^2 \rho(r)$, when combined with high values of $\rho(r)$, indicate covalent character in the bonding region. Positive values of $\nabla^2 \rho(r)$ indicate excess kinetic energy density over potential energy density, which is signal of either ionic or charge-shifted character. One other parameter of interest is the ratio $-(G(r_b)/V(r_b))$. $G(r_b)$ refers to the Lagrangian kinetic energy, while the value $V(r_b)$ is a measure of the potential energy density. $-(G(r_b)/V(r_b))$ ratio values higher than 1 indicate a noncovalent bond, while between 0.5 and 1 the bond is partially covalent. Ratio below 0.5 indicates fully covalent bonding.

The values of these parameters for all studied compounds are found on **Table 1**. All the studied bonds are found to be fully covalent, as they all show negative values for $\nabla^2 \rho(r)$ and high $\rho(r)$, besides $-(G(r_b)/V(r_b))$ ratio values lower than 0.5. No visible trend is found by replacing the peroxide bond with other types of bonds. Namely, while **1a** and **1c** present higher $\rho(r)$ than **1b**, the $-(G(r_b)/V(r_b))$ ratio is similar for **1b** and **1c** (being lower than for **1a**). $\nabla^2 \rho(r)$ is also similar between **1a** and **1b**, but lower than **1c**. **1d** present values somewhat difference than the ones found for **1a-c**, which can be explained for this BCP not being related to a heteroatomic bond. Given this, the insight provided by analysing the target bonds at the reactant geometry appears to be limited, indicating that analysing the thermolysis and chemiexcitation steps is essential.

Table 2 – Activation energies ($\Delta E(\ddagger)$, in kcal mol⁻¹) and energetic difference between products and reactants ($\Delta E(r)$, in kcal mol⁻¹), for the thermolysis reaction of model dioxetanone and its 3 non-peroxide derivatives, at the ω B97XD/6-31+G(d,p) level of theory.

Molecule	$\Delta E(\ddagger)$	$\Delta E(r)$
1a	24.0	-79.9
1b	53.1	-1.1
1c	50.9	-13.0
1d	55.6	29.9

So, we proceeded to study the thermolysis reactions of **1a-d**. **Figure 1** shows the potential energy curves for the thermolysis of the four studied structures (**Scheme 1**), which are composed of the energies of S_0 and S_1 as a function of intrinsic reaction coordinates. The activation energy ($\Delta E(\ddagger)$) and the S_0 energy difference between products and reactants ($\Delta E(r)$) are presented in **Table 2**.

Interestingly, only the thermolysis of **1a** appears to be energetically favourable, as the reaction is highly exothermic (-79.9 kcal mol⁻¹) with a relatively small activation energy (24.0 kcal mol⁻¹). This is fully in line with previous data for the thermolysis of dioxetanones.^{15,35,37,39,40-43} Both **1b** and **1c** are also exothermic, but to a lesser degree (-1.1 and -13.0 kcal mol⁻¹, respectively). However, both present quite high activation energies, in the order of ~ 50 kcal mol⁻¹ (**Table 1**). The thermolysis of **1d** is clearly unfavourable, as it is both endothermic (29.9 kcal mol⁻¹) and possesses a significantly high activation energy (55.6 kcal mol⁻¹).

There are also important differences between molecules regarding the thermolysis reaction mechanism, as evidenced by the analysis of the evolution of -O-O/-S-S/-HN-NH/-H₂C-CH₂- and -C-C- bond length of the four-membered cyclic structures during thermolysis (**Figure S1**), as well as by the variation of $\langle S^2 \rangle$ as a function on intrinsic reaction coordinates (**Figure S2**).

The thermolysis of **1a** proceeds via a stepwise biradical mechanism, which is consistent with previous data.^{15,35,37,39,40-43} This is indicated by the determination of $\langle S^2 \rangle$ values of ~ 1.0 during the thermolysis reaction (**Figure S2**), as well as by the sequential breaking of -O-O- and -C-C- bonds (**Figure S1.A**). As for both **1c** and **1d**, $\langle S^2 \rangle$ is always zero, indicating the absence of a biradical during this reaction (**Figure S2**). Furthermore, the breaking of -HN-NH/-H₂C-CH₂- and C-C bonds is concerted and not stepwise (**Figures S1.C** and **S1.D**). The thermolysis reaction mechanism of **1b** is somewhat an intermediate between that of **1a** and **1c/1d**. More specifically, while there is no evidence of the presence of a biradical (as for **1c/1d**), there is small open-shell character for **1b** near the TS, with $\langle S^2 \rangle$ values of ~ 0.1 (**Figure S2**). Finally, the bond length variation in -S-S- and -C-C- is more merged than either fully concerted or fully stepwise (**Figure S1.B**).

Having reached this point, it is time to note that the results already show significant differences between the thermolysis reaction of model dioxetanone **1a** and derivatives **1b-d**. Namely, only the S_0 thermolysis reaction of **1a** appears to be energetically favourable. Given that $S_0 \rightarrow S_1$ chemiexcitation only occurs during the thermolysis of dioxetanone,¹⁻³ these results indicate that only **1a** could potentially lead to efficient CL. Nevertheless, this alone does not exclude the possibility for efficient $S_0 \rightarrow S_1$ chemiexcitation during the energetically unfavourable thermolysis of **1b-d**. Thus, the next step of this work was to evaluate the $S_0 \rightarrow S_1$ interplay during the thermolysis reaction of the studied molecules (**Figure 1**).

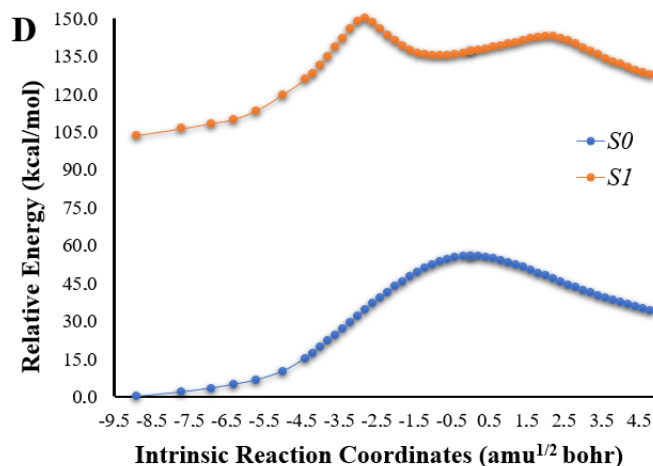
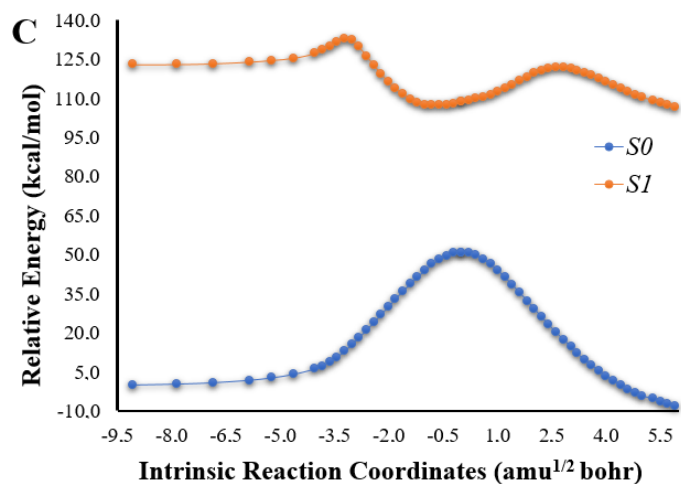
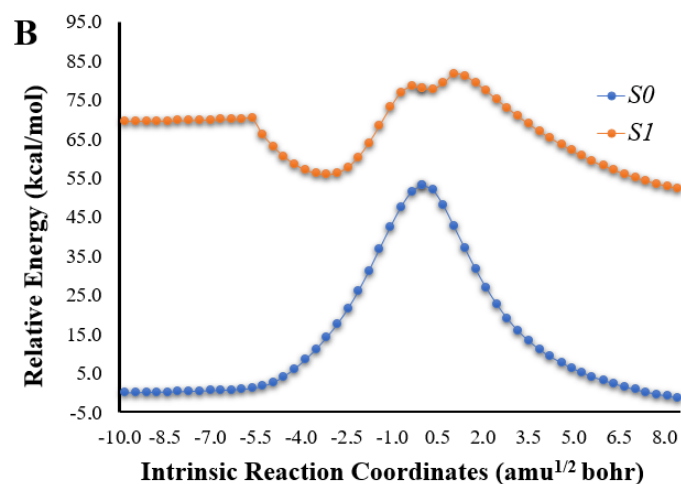
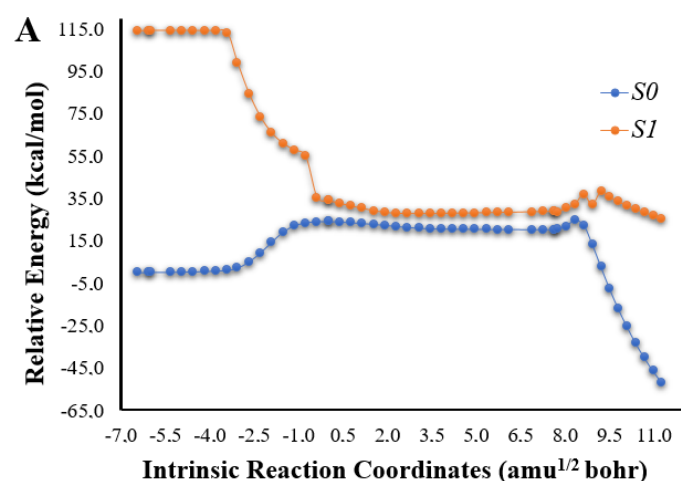


Figure 1 – Potential energy curves of S_0 and S_1 states as a function of intrinsic reaction coordinates of **1a** (A), **1b** (B), **1c** (C) and **1d** (D). The curves were calculated at the ω B97XD/6-31+G(d,p) level of theory.

The calculations indicate that during the thermolysis of **1a** there is a large and flat region of the PES, within the biradical region, in which S_0 and S_1 are degenerated/nearly degenerated (**Figure 1.A**). More specifically, while the energy difference between S_0 and S_1 is of 114.0 kcal mol⁻¹ at the start of the reaction, it decreases significantly to 6.1–11.3 kcal mol⁻¹ between intrinsic reaction coordinates of -0.4 and 8.3 amu^{1/2} bohr. This type of energetic profile, in which there is degeneracy between states during a large and flat region of the PES, can be associated with efficient chemiexcitation, as there are near-infinite possibilities for non-adiabatic transitions.^{36,37,39,53,54} It should be noted that previous results indicate that multireference calculations should predict even smaller S_0 - S_1 energy gaps.^{36,37,39,53,54} This results from the importance of multireference correlation in these systems, with the energetic error present in this region in the TD-DFT approach resulting from spin contamination in the reference state by the use of BS technology.³⁵⁻³⁷ However, multireference calculations can be quite expensive in terms of computational power, and previous results also demonstrated that multireference and TD-DFT calculations only differ in quantitative terms for these systems, and not in qualitative ones.^{35-43,54}

Interestingly, while for **1b-d** the S_0 - S_1 energy gap is at the lowest near its respective TS, the results clearly indicate that there is no available $S_0 \rightarrow S_1$ chemiexcitation pathway for any of the non-peroxide derivatives (**Figures 1.B-1.D**). More specifically, the lowest S_0 - S_1 energy gap for each molecule is still too high to allow for efficient chemiexcitation: 24.7 kcal mol⁻¹ for **1b**, 57.5 kcal mol⁻¹ for **1c**, and 80.6 kcal mol⁻¹ for **1d**. Thus, the results provide a negative answer to one of our starting questions: can dioxetanone derivatives with non-peroxide bonds also allow for chemiexcitation? The exchange of the peroxide bond for another type of bond (-S-S-, -HN-NH- and -H₂C-C₂H-) made the thermolysis reaction both energetically unfavourable and devoid of the $S_0 \rightarrow S_1$ chemiexcitation pathway. So, the next step of this work consisted in obtaining an answer to our second starting

question: why can the peroxide bond lead to chemiexcitation, while other types of bonds cannot?

One possible explanation could be related with existent theories for efficient chemiexcitation of dioxetanones and related peroxides, such as CTIL³⁵⁻³⁸ and/or CIEEL^{31,32}. That is, despite the flaws associated with these mechanisms (as described in the Introduction section), it could be possible that peroxide-based dioxetanones decomposed through them while non-peroxide-based derivatives were unable to do so. Given this, we have first tried to assess if the CTIL theory could be involved in thermolysis of **1a**, while being absent for **1b-d**. To this end, we have measured the NBO charge separation between the dioxetanone/non-peroxide derivative and the benzene moieties (**Figure 2**) for all molecules as a function of intrinsic reaction coordinates.

The results exclude the involvement of the CTIL mechanism in the thermolysis and subsequent chemiexcitation of **1a** (**Figure 2.A**). Namely, there is no relevant CT and BCT between the dioxetanone and the benzene moieties from the start of the reaction (-6.5 $\text{amu}^{1/2} \text{ bohr}$) to the end of the biradical region in which chemiexcitation is possible (8.3 $\text{amu}^{1/2} \text{ bohr}$). Only from 8.3 $\text{amu}^{1/2} \text{ bohr}$ onward is it possible to see some CT/BCT, but without any connection to chemiexcitation or the biradical region. The magnitude of charge separation between moieties is also quite small for the other studied molecules (**Figure 2.B-2.D**), which indicates that there are no relevant CT/BCT processes between the four-membered cycle and the electron-rich moiety for any of them. Thus, this is further evidence that the CTIL mechanism, as proposed, does not appear to be able to explain the chemiexcitation of cyclic peroxides, such as dioxetanone.

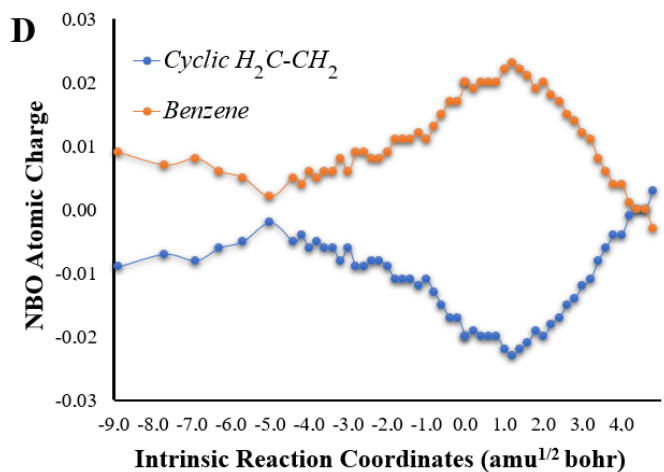
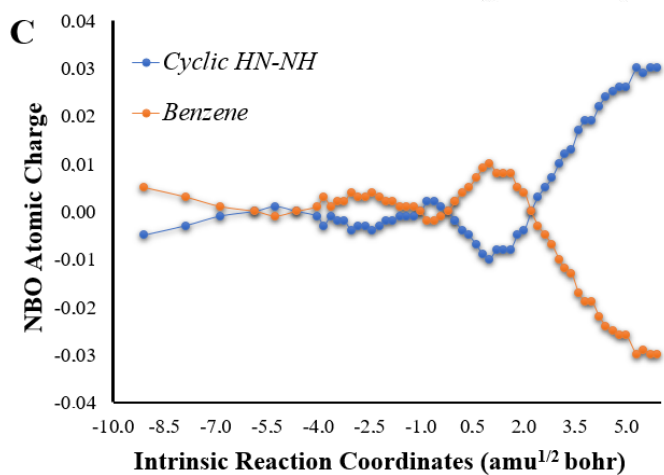
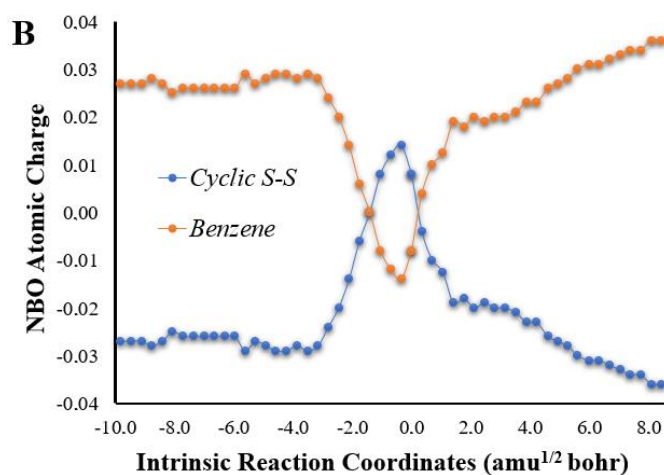
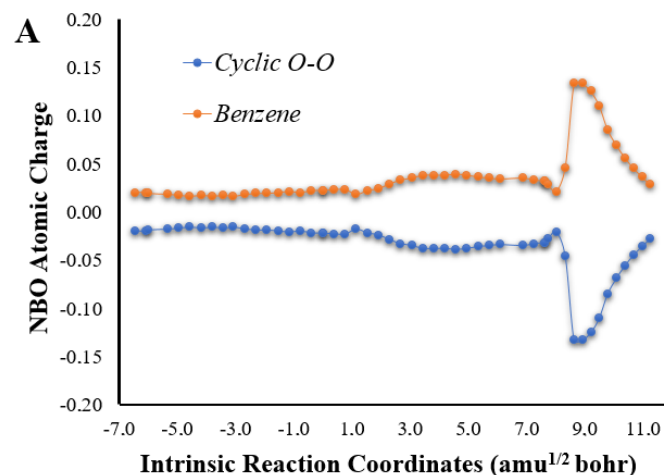


Figure 2 – NBO atomic charges as a function of intrinsic reaction coordinates of **1a** (A), **1b** (B), **1c** (C) and **1d** (D). The charge densities were calculated at the ω B97XD/6-31+G(d,p) level of theory.

The subsequent hypothesis would be the involvement of the CIEEL mechanism (ET/BCT between the peroxide ring and an electron-rich moiety, with formation of a radical pair)^{31,32} in the thermolysis of **1a**, while being absent in the thermolysis of **1b-1d**. This hypothesis could be more relevant, given that **1a** is both the only molecule to undergo thermolysis with formation of a biradical (**Figure S2**), and the only molecule which thermolysis allows for chemiexcitation (**Figure 1**). However, analysis of the

ARTICLE

electron spin density of the cyclic peroxide and benzene moieties (Figure S3.A) of **1a** revealed that there was not any relevant transfer of electron spin density between them. On the contrary, the formation of the biradical is due to the homolytic -O-O- bond breaking of the dioxetanone, with all the electron spin density residing in the two oxygen heteroatoms that compose this bond (Figure S3.B). This finding is in line with the results obtained for other dioxetanones.^{40-43,53,54}

In summary, our results demonstrate that neither CIEEL nor CTIL mechanisms can explain why peroxide-based heterocycles undergo chemiexcitation and the other types of studied heterocycles do not, given that these mechanisms were not applicable to the thermolysis of **1a**. Once again, these results also put into question both the CIEEL and CTIL mechanisms as possible explanations for the chemiexcitation of dioxetanone molecules, as they were not able to explain the chemiexcitation of the model peroxide (**1a**).

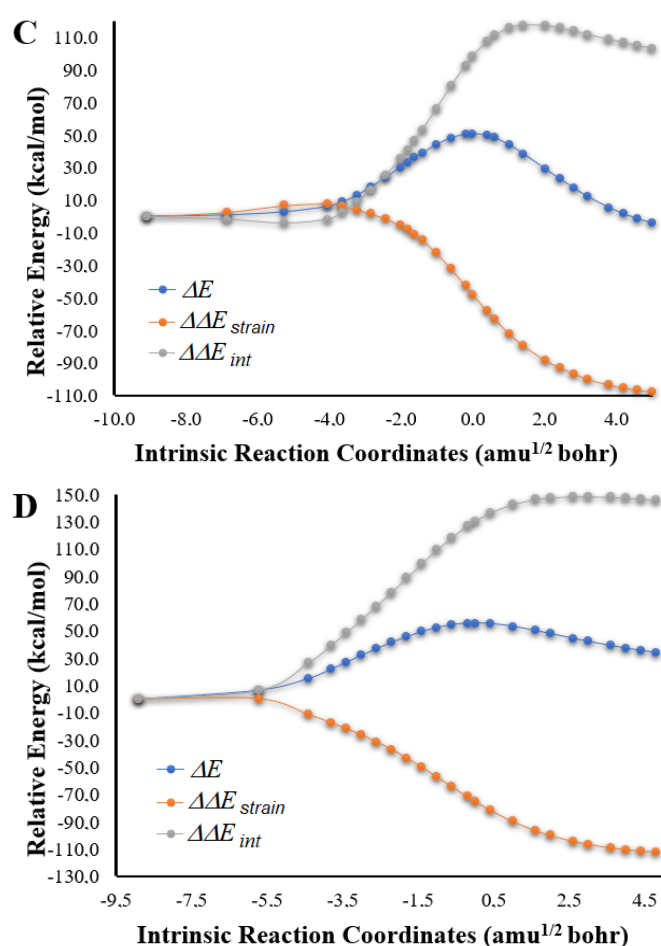
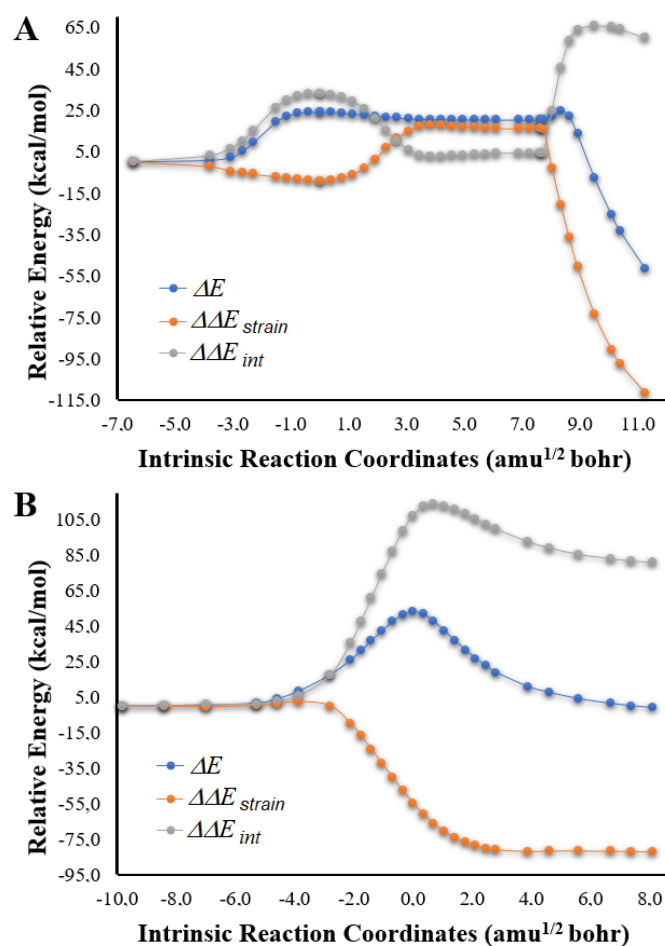


Figure 3 - $\Delta E(\zeta)$, $\Delta\Delta E(\zeta)_{strain}$ and $\Delta\Delta E(\zeta)_{int}$ values plotted as a function of intrinsic reaction coordinates for **1a** (A), **1b** (B), **1c** (C) and **1d** (D), calculated at the ω B97XD/6-31+G(d,p) level of theory.

Having said that, it is still unclear why the peroxide-based heterocycle can undergo chemiexcitation. The main difference between the thermolysis of **1a** and **1b-d** is the presence of a large and flat biradical region in the former reaction, in which S_0 and S_1 are degenerated/nearly-degenerated (allowing for chemiexcitation). Indeed, the presence of the biradical region can provide some explanation, since as the -O-O- bond breaks homolytically the σ and σ^* orbitals become lone-pair orbitals with each oxygen heteroatom retaining one electron of the original σ bond.^{49,53-55} These new O lone pairs become almost degenerate with the original O lone pairs (initially perpendicular to the ring plane), generating a manifold of four singlet and four triplet states.^{49,53-55} Thus, it makes sense that the presence of a biradical is necessary for the occurrence of efficient chemiexcitation in these systems. In fact, it should be noted that while **1b-d** do not present chemiexcitation (due to the absence of a biradical), **1b** presents the lowest S_0 - S_1 energy gap of the three molecules (~ 24 versus ~ 58 - 80 kcal mol⁻¹) and that it occurs at a point of small open-shell character (Figures 1 and S2).

However, though the presence of a biradical might be a requisite for accessing the large and flat region of the PES where S_0 and S_1 are degenerated/nearly-degenerate, its presence alone is not enough. More specifically, while all dioxetanones appear to undergo thermolysis via a stepwise biradical mechanism, not all of them undergo efficient chemiexcitation: some undergo thermolysis by accessing a long and flat biradical PES region of S_0 - S_1 degeneracy whereas others undergo decomposition without having access to such degeneracy region (despite the reaction also occurring through a biradical region of the PES).^{39-43,54} It should be noted that although anionic dioxetanones do not seem to have access to this region of degeneracy in general (in which the biradical is formed by ET between the peroxide and the electron-rich moiety),³⁵⁻⁴³ for neutral dioxetanones (in which the biradical is typically formed by homolytic bond breaking) the access to the degeneracy region seems to depend on the functionalization of the cyclic peroxide structure.^{43,54}

Recent studies of our group have correlated the access to this region of degeneracy to increasing attractive interactions between the CO_2 and keto fragments (**Scheme 1**) of the thermolysis of dioxetanone, which delays CO_2 detachment.^{39,41,54} This phenomenon enables the reacting molecules to spend more time on the biradical region of the PES, thereby reaching the region of S_0 - S_1 degeneracy and increasing the probabilities for chemiexcitation.^{39,41,54} Dioxetanone species without increased attractive interactions between the fragments eject CO_2 quickly, and so, do not have access to the region of degeneracy.^{39,41,54}

To verify if this hypothesis is related with the thermolysis/chemiexcitation of **1a**, and if this increased interaction also occurs during the thermolysis of **1b-d**, we have used the activation strain model⁵⁶⁻⁵⁸ to evaluate the evolution of the interaction energy during the reactions. This model decomposes the potential energy surface $\Delta E(\zeta)$ into two main contributions along the reaction coordinate ζ : the reaction strain ($\Delta E(\zeta)_{\text{strain}}$), which is determined by the structural distortion that the reactants suffer during the reaction; and $\Delta E(\zeta)_{\text{int}}$, which consists in the interaction energy between the reactants. Thus, $\Delta E(\zeta)_{\text{int}}$ results from the bonding capabilities and mutual interactions between the reactants along the reaction coordinate. As dioxetanones's thermolysis is a unimolecular reaction, this analysis will not be between the reactants but between the resulting fragments of the thermolysis reactions (**Scheme 1**).

The values of $\Delta E(\zeta)$, $\Delta\Delta E(\zeta)_{\text{strain}}$ and $\Delta E(\zeta)_{\text{int}}$ are plotted as a function of intrinsic reaction coordinates for all species (**Figure 3**), where $\Delta\Delta E(\zeta)_{\text{strain}}$ is the sum of the $\Delta E(\zeta)_{\text{strain}}$ for both fragments and $\Delta\Delta E(\zeta)_{\text{int}}$ is the change of $\Delta E(\zeta)_{\text{int}}$ as a function of the intrinsic reaction coordinates, with the $\Delta E(\zeta)_{\text{int}}$ of the reactant as reference. Interestingly, there are two types of energetic profiles, one for **1a** and another for **1b-d**. The energetic

profile of **1b-d** is similar to that found for model dioxetanones with inefficient chemiexcitation.⁵⁴ Namely, $\Delta\Delta E(\zeta)_{\text{strain}}$ is increasingly negative and $\Delta\Delta E(\zeta)_{\text{int}}$ increasingly positive (**Figures 3.B-3.D**). The former indicates that the four-membered ring is under significant strain, and that thermolysis reduces it. The latter indicates that thermolysis leads to increasing repulsion between the two generated fragments, what is consistent with our previously defined hypothesis, in which repulsive interactions between fragments reduce the length of the biradical region and prevent access to a region of degeneracy.^{39,41,54}

On the contrary, the energetic profile found for **1a** is in line with what was found before for other model dioxetanones with efficient chemiexcitation pathways (**Figure 3.A**).⁵⁴ That is, the analysis with the activation strain model allows the thermolysis energy profile to be divided into three phases. The first phase (from reactant to TS) is identical to that of other thermolysis reactions, in which $\Delta\Delta E(\zeta)_{\text{strain}}$ is increasingly negative and $\Delta\Delta E(\zeta)_{\text{int}}$ increasingly positive. However, after the TS and upon entering the biradical region, the interaction between fragments becomes attractive (decrease of $\Delta\Delta E(\zeta)_{\text{int}}$) until reaching the point of -C-C- bond breaking (**Figure 3.A**). This initiates the final phase of the reaction, in which $\Delta\Delta E(\zeta)_{\text{strain}}$ is once again increasingly negative and $\Delta\Delta E(\zeta)_{\text{int}}$ increasingly positive.

To further analyse the differences relative to fragment interaction for the four studied reactions, we have also plotted their $\Delta E(\zeta)_{\text{int}}$ variations as a function of intrinsic reaction coordinates (**Figure 4.A**). For **1b-d**, there is increasing repulsion between fragments up until the TS, noticeable by $\Delta E(\zeta)_{\text{int}}$ reaching positive values. Given that for these molecules the TS also corresponds to -C-C- bond breaking, after that, $\Delta E(\zeta)_{\text{int}}$ starts to decrease to neutral values as the fragments are too separated to interact in a relevant manner. However, for **1a**, $\Delta E(\zeta)_{\text{int}}$ inverts its ascent into positive values at the TS, with this parameter becoming increasingly negative in the biradical region. Only after -C-C- bond scission does $\Delta E(\zeta)_{\text{int}}$ reflect the occurrence of repulsive interactions between fragments. Given this, these results support our hypothesis, in which the biradical region is extended for certain dioxetanones, due to attractive interactions between reaction fragments that delay CO_2 detachment, and allows for access to the region of S_0 - S_1 degeneracy.⁵⁴

It should be noted that in the second phase of the thermolysis of **1a**, $\Delta\Delta E(\zeta)_{\text{strain}}$ also becomes less negative (**Figure 3.A**). This has been attributed before to increasing strain in the CO_2 fragment in this extended region of biradical character, given that geometrical modifications without possibility for -C-C- bond scission increase its strain in a relevant manner.⁵⁴

Having reached this point, our results indicate that the reasons why **1a** appears to have access to an efficient chemiexcitation pathway (as opposed to non-peroxide derivatives) are the

presence of a biradical region during its thermolysis and attractive interactions between reaction fragments that provide access to a region of degeneracy between states. Given this, further insight must be gained on why there is increasing interaction between fragments for **1a** yet not for non-peroxide derivatives **1b-d**.

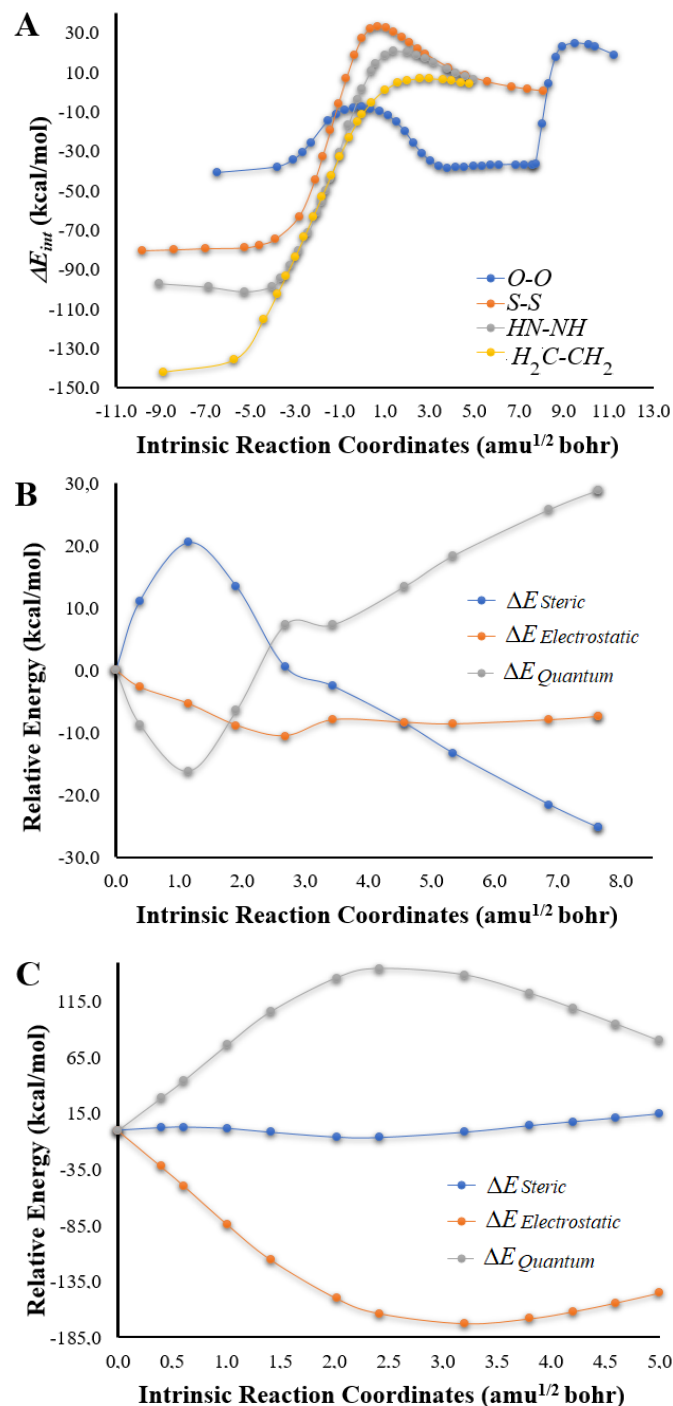


Figure 4 - $\Delta E(\zeta)_{int}$ values plotted as a function of intrinsic reaction coordinates for **1a-d** (A). Energy decomposition of the total molecular energy of **1a** (B) and **1c** (C) into ΔE_{Steric} , $\Delta E_{Quantum}$ and $\Delta E_{Electrostatic}$ as a function of the intrinsic reaction coordinates of their thermolysis reaction.

The first studies by our group on this topic have indicated that for imidazopyrazinone-based dioxetanones (as for the Coelenterazine and *Cypridina* luciferin systems) an important parameter should be attractive electrostatic interactions between fragments given the existence of relevant charge separation between the keto and CO_2 fragments for those molecules.^{39,41} Our subsequent study, also indicated that attractive electrostatic interactions should be a relevant parameter for dioxetanone species, given that model dioxetanones with efficient chemiexcitation presented higher charge separation between fragments than other dioxetanones lacking efficient chemiexcitation.⁵⁴ However, in that study, we have also analysed other types of cyclic peroxide molecules (model dioxetanes) and found that, for those systems, electrostatic interaction does not appear to be very relevant for the attractive interactions that occur during the biradical region of degeneracy.⁵⁴ Thus, there is some doubt on whether electrostatic interactions are relevant for all dioxetanones but not for dioxetanes, or if electrostatic interactions only contribute for increasing attractive interactions in some cases, even within the dioxetanone class of molecules.

To try to overcome these doubts, we have also measured the charge separation between the fragments that result from the thermolysis of **1a** and **1c**, as a comparison reference (Figure S4). Contrary to what was found for other dioxetanones, there is no relevant charge separation (only $\sim 0.02e$ within the biradical region) that could indicate a role for electrostatic interactions during the thermolysis of **1a**. Thus, electrostatic interactions do not seem the main contributor for the increased attractive interactions between thermolysis fragments of cyclic peroxides with efficient chemiexcitation.⁵⁴ Nevertheless, they should contribute in some systems with relevant charge separation between fragments, such as the imidazopyrazinone-based systems.^{39,41} As for **1c**, while there is some charge separation at the beginning of the reaction, it quickly decreases to neutral values.

Given the apparent irrelevance of electrostatic interaction in the **1a** system, we proceeded to decompose the total energy of the system (as a function of intrinsic reaction coordinates of the thermolysis reaction) into three different parameters (Figure 4.B) by using the Shubin Liu's energy decomposition scheme.⁵⁹ In it, the total molecular energy is decomposed into: E_{Steric} , which is the energy derived by Weizsäcker kinetic functional; $E_{Electrostatic}$, which is the sum of all classical Coulomb interactions of the particles in the system; $E_{Quantum}$, which is the energy purely caused by quantum effects that essentially exhibits electronic correlation effects as well as influence of the Pauli exclusion principle on electronic kinetic energy under non-interacting particle assumption.^{59,60} The energy decomposition was performed with the Multiwfn 3.8 software⁶⁰ and based on the DFT calculations performed with Gaussian 09. This analysis was just made for the biradical region, which is the one of interest for the increasing attractive interactions. For

comparison purposes, a similar analysis was made for **1c**, from the TS onward (Figure 4.C). It should be noted that the presented values are not absolute energy values (E_{Steric} , $E_{Electrostatic}$, and $E_{Quantum}$), but instead the variation of these energy values as a function of intrinsic reaction coordinates (ΔE_{Steric} , $\Delta E_{Electrostatic}$, and $\Delta E_{Quantum}$).

For **1a** (Figure 4.B), within the biradical region, the total energy of the system is dominated by ΔE_{Steric} and $\Delta E_{Quantum}$, with $\Delta E_{Electrostatic}$ providing less relevant negative contributions. It should be noted, however, that while ΔE_{Steric} and $\Delta E_{Quantum}$ start by providing positive and negative contributions (respectively) to the total molecular energy, they quickly start to provide opposite contributions (negative and positive, respectively). This inversion occurs in the same region of the PES in which ΔE_{int} stops becoming less negative and starts to become increasingly negative again (~ 0.0 - 3.0 amu^{1/2} bohr, Figure 4.A). So, the results indicate that the increasing attractive interactions that delay the thermolysis of dioxetanone **1a** result from increasing negative contributions of ΔE_{Steric} that, along with moderate contributions from $\Delta E_{Electrostatic}$, offset increasing positive contributions of $\Delta E_{Quantum}$.

Analysis of the evolution of the total molecular energy of **1c** provides a different profile (Figure 4.D), as now the energy is dominated by negative contributions of $\Delta E_{Electrostatic}$ and positive contributions of $\Delta E_{Quantum}$, while ΔE_{Steric} provides comparatively smaller positive contributions. This shows that there is indeed a different behaviour of ΔE_{Steric} within the biradical region of the thermolysis of **1a**, which can help to understand why there are increasing attractive interactions between the reaction fragments that extend the biradical region of degeneracy. Thus, future steps in this topic of research should be subsequent studies regarding the different contributing factors that govern the interaction energy between the fragments of the thermolysis reaction of CL-capable cyclic peroxides.

Conclusions

We have investigated the fundamentals of the chemiexcitation process of a dioxetanone model system by replacing the peroxide bond with other types of bonds (sulphur-sulphur, nitrogen-nitrogen, and carbon-carbon) and employing a TD-DFT approach. We have found that while model dioxetanone undergoes thermolysis via a stepwise biradical mechanism, the thermolysis of studied non-peroxide derivatives proceeds via a concerted mechanism. Furthermore, the thermolysis of the former is the only energetically favourable reaction, being highly exothermic. On the contrary, the other reactions proceed with significantly high activation barriers while being only slightly exothermic or even endothermic. Finally, while the decomposition of the model dioxetanones provides a pathway for efficient singlet chemiexcitation, the thermolysis of the non-peroxide derivatives does not.

Singlet chemiexcitation of the model dioxetanone is explained by the presence of a large and flat biradical region during the thermolysis reaction, in which both the ground and singlet excited state are degenerated. Access to this region is achieved through increasing attractive interactions between the resulting thermolysis fragments, which delay the rupture of the peroxide ring and allow the reacting molecule to spend more time in the region of degeneracy (increasing the probabilities for chemiexcitation). There was no evidence of the involvement of neither the CIEEL nor the CTIL mechanisms in the chemiexcitation of this molecule.

Summarizing, our results indicated that replacing the peroxide bond in the dioxetanone structure with either sulphur-sulphur, nitrogen-nitrogen, or carbon-carbon bonds prevents the occurrence of chemiluminescence. Namely, this type of structural replacement turns the thermolysis reaction into an energetically unfavourable process, while eliminating the pathway for singlet chemiexcitation. Comparative analysis between the chemiexcitation of model dioxetanone and the non-peroxide derivatives provided insight into the fundamentals of this process.

Conflicts of interest

There are no conflicts to declare.

Acknowledgements

This work was made in the framework of the project PTDC/QUI-QFI/2870/2020, funded by the Portuguese Foundation for Science and Technology (FCT, Lisbon). Acknowledgments are also made to UIDB/00081/2020 and UIDB/05748/2020. Luís Pinto da Silva acknowledges funding from the Portuguese Foundation for Science and Technology (FCT, Lisbon), under the Scientific Employment Stimulus (CEECIND/01425/2017). Carla M. Magalhães acknowledges funding from FCT for her PhD grant (SFRH/BD/143211/2019). Patricia González-Berdullas acknowledges FCT for funding her post-Doc position under project PTDC/QUI-QFI/2870/2020. The Laboratory of Computational Modelling of Environmental Pollutants-Human Interactions (LACOMEPI) is acknowledged.

References

- 1 L. Pinto da Silva and J.C.G. Esteves da Silva, *ChemPhysChem*, 2012, **13**, 2257.
- 2 M. Matsumoto, *J. Photochem. Photobiol. C*, 2004, **5**, 27.
- 3 M. Vacher, I.F. Galván, B.W. Ding, S. Schramm, R. Berraud-Pache, P. Naumov, N. Ferré, Y.J. Liu, I. Navizet, D. Roca-Sanjuán, W.J. Baader and R. Lindh. *Chem. Rev.*, 2018, **118**, 6927.
- 4 F.A. Augusto, G.A. Souza, S.P. Souza Júnior, M. Khalid and W.J. Baader, *Photochem. Photobiol.*, 2013, **89**, 1299.
- 5 L. Pinto da Silva and J.C.G. Esteves da Silva, *Chem. Phys. Lett.*, 2014, **608**, 45.
- 6 C. Carrasco-López, N.M. Lui, S. Schramm and P. Naumov, *Nat. Rev. Chem.*, 2021, **5**, 4.

- 7 N.S. Rodionova, E. Rota, A.S. Tsarkova and V.N. Petushkov, *Photochem. Photobiol.*, 2017, **93**, 416.
- 8 S. Gnaim, D. Green and D. Shabat, *Chem. Commun.*, 2018, **54**, 2073.
- 9 S. Gnaim and D. Shabat, *J. Am. Chem. Soc.*, 2017, **139**, 10002.
- 10 K.K. Krzyminski, A.D. Roshal, P.B. Rudnicki-Velasquez and K. Zamojc, *Luminescence*, 2019, **34**, 512.
- 11 S.M. Marques, F. Peralta and J.C.G. Esteves da Silva, *Talanta*, 2009, **77**, 1497.
- 12 M. Cronin, A.R. Akin, K.P. Francis and M. Tangney, *Methods Mol. Biol.*, 2016, **1409**, 69.
- 13 K.M. Grinstead, L. Rowe, C.M. Ensor, S. Joel, P. Daftarian, E. Dikici and S. Daunert, *PLoS One*, 2016, **11**, e0158579.
- 14 M.J. Hsu, J. Prigent, P.E. Dollet, J. Ravau, L. Larbanoix, F.G. Van Simaey, A. Bol, S. Goldman, G. Deblandre, M. Najimi, E. Sokal and C. Lombard, *Stem Cells Dev.*, 2017, **26**, 986.
- 15 L. Pinto da Silva, A. Núñez-Montenegro, C.M. Magalhães, P.J.O. Ferreira, D. Duarte, P. González-Berdullas, J.E. Rodríguez-Borges, N. Vale, J.C.G. Esteves da Silva, *Eur. J. Med. Chem.*, 2019, **183**, 111683.
- 16 L. Pinto da Silva, C.M. Magalhães, A. Núñez-Montenegro, P.J.O. Ferreira, D. Duarte, J.E. Rodríguez-Borges, N. Vale, J.C.G. Esteves da Silva, *Biomolecules*, 2019, **9**, 384.
- 17 C.M. Magalhães, J.C.G. Esteves da Silva and L. Pinto da Silva, *ChemPhysChem*, 2016, **17**, 2286.
- 18 A. Boaro, R.A. Reis, C.S. Silva, D.U. Melo, A.G.G.C. Pinto and F.H. Bartoloni, *J. Org. Chem.*, 2021, DOI: 10.1021/acs.joc.1c00230.
- 19 H. Kondo, T. Igarashi, S. Maki, H. Niwa, H. Ikeda and T. Hirano, *Tetrahedron Lett.*, 2005, **46**, 7701.
- 20 F.A. Augusto, F.H. Bartoloni, A.P.E. Pagano and W.J. Baader, *Photochem. Photobiol.*, 2021, **97**, 309.
- 21 A. Giussani, P. Farahani, D. Martínez-Munoz, M. Lundberg, R. Lindh and D. Roca-Sanjuán, *Chem. Eur. J.*, 2019, **25**, 5202.
- 22 C. Garcia-Irepa, M. Marazzi and I. Navizet, *Phys. Chem. Chem. Phys.*, 2020, **22**, 26787.
- 23 S. Schramm, I. Navizet, D.P. Karoathy, P. Oesau, V. Bensmann, D. Weiss, R. Beckert, P. Naumov, *Phys. Chem. Chem. Phys.*, 2017, **19**, 22852.
- 24 M. Nakazono, Y. Oshikawa, M. Nakamura, H. Kubota, S. Nanbu, *J. Org. Chem.*, 2017, **82**, 2450.
- 25 J. Czechowaska, A. Kawecka, A. Romanowska, M. Marczak, P. Wityk, K. Krzyminski, B. Zadykiewicz, *J. Lumin.*, 2017, **187**, 102.
- 26 L.F.M.L. Ciscato, F.H. Bartoloni, A.S. Colavite, D. Weiss, R. Beckert, S. Schramm, *Photochem. Photobiol. Sci.*, 2014, **13**, 32.
- 27 Z.M. Kaskova, A.S. Tsarkova and I.V. Yampolsky, *Chem. Soc. Rev.*, 2016, **45**, 6048.
- 28 R. Berraud-Pache, R. Lindh and I. Navizet, *J. Phys. Chem. B*, 2018, **122**, 5173.
- 29 C.G. Min, Q.B. Liu, Y. Leng, C.M. Magalhães, S.J. Huang, C.X. Liu, X.K. Yang and L. Pinto da Silva, *J. Chem. Inf. Model.*, 2019, **59**, 4393.
- 30 C.M. Magalhães, J.C.G. Esteves da Silva and L. Pinto da Silva, *J. Photochem. Photobiol. B*, 2019, **190**, 21.
- 31 J.Y. Koo and G.B. Schuster, *J. Am. Chem. Soc.*, 1977, **99**, 6107.
- 32 J.Y. Koo and G.B. Schuster, *J. Am. Chem. Soc.*, 1978, **100**, 4496.
- 33 L.H. Catalani and T. Wilson, *J. Am. Chem. Soc.*, 1989, **111**, 2633.
- 34 M.A. Oliveira and F.H. Bartoloni, F.A. Augusto, L.F.M.L. Ciscato, E.L. Bastos, W.J. Baader, *J. Org. Chem.*, 2012, **77**, 10537.
- 35 B.W. Ding and Y.J. Liu, *J. Am. Chem. Soc.*, 2017, **139**, 1106.
- 36 L. Yue, Y.J. Liu and W.H. Fang, *J. Am. Chem. Soc.*, 2012, **134**, 11632.
- 37 B.W. Ding, P. Naumov and Y.J. Liu, *J. Chem. Theory Comput.*, 2015, **11**, 591.
- 38 H. Isobe, Y. Takano, M. Okumura, S. Kuramitsu and K. Yamaguchi, *J. Am. Chem. Soc.*, 2005, **127**, 8667.
- 39 L. Pinto da Silva, R.F.J. Pereira, C.M. Magalhães and J.C.G. Esteves da Silva, *J. Phys. Chem. B*, 2017, **121**, 7862.
- 40 C.G. Min, P.J.O. Ferreira and L. Pinto da Silva, *J. Photochem. Photobiol. B*, 2017, **174**, 18.
- 41 C.M. Magalhães, J.C.G. and L. Pinto da Silva, *J. Lumin.*, 2018, **199**, 339.
- 42 L. Pinto da Silva, C.M. Magalhães and J.C.G. Esteves da Silva, *ChemistrySelect*, 2016, **1**, 3343.
- 43 L. Pinto da Silva, C.M. Magalhães, D.M.A. Crista and J.C.G. Esteves da Silva, *Photochem. Photobiol. Sci.*, 2017, **16**, 897.
- 44 T. Hirano, Y. Takahashi, H. Kondo, S. Maki, S. Kojima, H. Ikeda and H. Niwa, *Photochem. Photobiol. Sci.*, 2008, **7**, 197.
- 45 Y. Takahashi, H. Kondo, S. Maki, H. Niwa, H. Ikeda and T. Hirano, *Tetrahedron Lett.*, 2006, **47**, 6057.
- 46 R. Saito, T. Hirano, S. Maki and H. Niwa, *J. Photochem. Photobiol. A*, 2014, **293**, 12.
- 47 A.R. Katritzky, C.A. Ramsden, J.A. Joule and V.V. Zhdankin, *Handbook of heterocyclic chemistry*, Elsevier, **2010**.
- 48 T. Eicher, S. Hauptmann and A. Speicher, *The Chemistry of Heterocycles: Structures, Reactions, Synthesis, and Applications*, John Wiley & Sons, **2013**.
- 49 I.F. Galván, H. Gustafsson and M. Vacher, *Photochem.*, 2019, **3**, 957.
- 50 J.D. Chai and M. Head-Gordon, *Phys. Chem. Chem. Phys.*, 2008, **10**, 6615.
- 51 C. Adamo and D. Jacquemin, *Chem. Soc. Rev.*, 2013, **43**, 845.
- 52 Gaussian 09, Revision D.01, M.J. Frisch et al., Gaussian, Inc., Wallingford CT, 2013.
- 53 L. De Vico, Y.J. Liu, J.W. Krogh and R. Lindh, *J. Phys. Chem. A*, 2007, **111**, 8013.
- 54 L. Pinto da Silva and C.M. Magalhães, *Int. J. Quantum Chem.*, 2019, **119**, e25881.
- 55 S. Wilsey, F. Bernardi, M. Olivucci, M.A. Robb, S. Murphy and W. Adam, *J. Phys. Chem. A*, 1999, **103**, 1669.
- 56 L.P. Wolters and F.M. Bickelhaupt, *WIREs Comput. Mol. Sci.*, 2015, **5**, 324.
- 57 D.H. Ess and K.N. Houk, *J. Am. Chem. Soc.*, 2007, **129**, 10646.
- 58 F.M. Bickelhaupt and K.N. Houk, *Angew. Chem. Int. Ed.*, 2017, **56**, 10070.
- 59 S. Liu, *J. Chem. Phys.*, 2007, **126**, 244103.
- 60 T. Lu and F. Chen, *J. Comput. Chem.*, 2012, **33**, 580.